Runoff Generation from Water Repellent Soils with High Spatial and Temporal Variability in Infiltration Capacity

Sheridan, G.J. [1, 2,3], P.N.J Lane[1, 2,3] , P.J. Noske[1] , C.B. Sherwin[1] and P. Nyman[1]

[1] School of Forest and Ecosystem Science, the University of Melbourne, Victoria
[2]eWater Cooperative Research Centre
[3]Cooperative Research Centre for Forestry

Email: sheridan@unimelb.edu.au

Keywords: *hydrology, water quality, soil erosion, saturated conductivity, forests*

EXTENDED ABSTRACT

Sheridan et al. (2007) reported that infiltration-excess runoff ratios of up to 60% were observed during 100 mm h^{-1} rainfall simulation on water repellent macroporous, clay loam forest soils in a SE Australian Eucalypt forest. At the same time, ponded ring infiltrometer measurements showed conductivities in the order of 100's of mm h^{-1}. The aim of this research is to test the hypothesis that these unusual results are due to strong water repellence resulting in very high spatial variability in conductivity, with a large proportion of soil surface area having zero to very low conductivity, punctuated by small areas of extremely high conductivity.

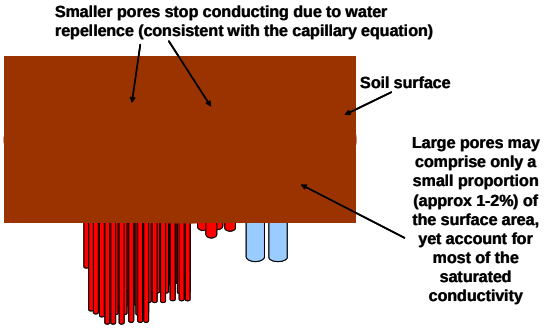

Figure 1. An illustration of how water repellence may lead to large runoff producing areas punctuated by small areas of very high conductivity.

Pore size distributions of intact soil cores were quantified at high soil water potentials (0-50cm water) using a tension table, while the relative contribution of these pore size classes to total conductivity were measured using tension infiltrometers in the field, also at water potentials close to zero. The results were used to generate a randomly arranged grid of relative conductivity with correct distribution properties for numerical simulations of runoff generation under 100 mm h^{-1} rainfall. These random grids of relative conductivity were then modified to prevent water entry to pores less than a critical diameter, based on the capillary equation and laboratory measurement of the soil-water contact angle of the water repellent soil. These modelled runoff values were compared to measured runoff from field 1.5 m wide rainfall simulation plots at 100 mm h^{-1} intensity and plot lengths between 0.1-2.0m.

The results showed that:

- Under non-water repellent conditions only a small fringe adjacent to the plot outlet contributes runoff to the plot exit;
- Both the runoff rate and the average connected length (with the plot outlet) are very sensitive to the selected contact angle;
- 20% runoff can be generated even when the infiltration capacity (127 mm h^{-1}) is higher than the rainfall rate (100 mm h^{-1}), if the contact angle is assumed to be 94°.

When the laboratory measured contact angle of 90.3° is used in the runoff model, runoff generation is increased only slightly in summer and the modelled results do not support the experimental hypothesis. However if it is assumed that the field soil-water contact angle increases to 94° in summer, then the results support the hypothesis that the observed spatial and temporal patterns of infiltration and runoff generation can be attributed to seasonal changes in water repellence. Several technical and theoretical issues may have bearing on the conclusions drawn from this paper.

The results have implications for infiltration-excess runoff estimation from areas with highly spatially variable conductivity, as are commonly found in forested environments, particularly where water repellence also occurs.

1. BACKGROUND

Infiltration excess overland flow is a key mechanism for transporting soil and pollutants from hillslopes to the stream network. Recent numerical simulations have illustrated the importance of spatial variability in soil hydraulic properties for infiltration-excess runoff generation (Morbidelli *et al.* 2006). The occurrence of water repellence in highly macroporous forest soils creates the potential for extreme spatial variability in infiltration rates, and hence an extreme example of the conditions simulated by Morbidelli *et al.* (2006). The implications of this variability with respect to runoff generation and soil erosion prediction in forests were explored by Shakesby *et al.* (2000). In particular, these authors note the limitations of scaling-up research results from point, to plot, and then to catchment scales when the landscape is characterised by highly variable "source" and "sink" areas for runoff and sediment. The experiments described in this paper aim to improve the prediction of the delivery of sediment and other pollutants to streams in forests that are characterised by the hydrologic conditions described above.

2. METHODS

2.1. Overview

Methods were selected to measure the soil pore size distribution and the relative saturated conductivity for different pore size classes so that runoff generation at different levels of water repellence could be estimated using computer simulations. Levels of water repellence were simulated by changing the soil water contact angle (the solid-liquid angle made when a drop of liquid sits on a solid). These modelled runoff generation results were compared to measured runoff from rainfall simulation plots during dry water-repellent conditions and wet non-water repellent conditions.

2.2. Pore size distribution

The pore size distribution was determined from the capillary equation (Eq 4). Six replicates of soil cores were collected in 73 mm diameter by 57 mm high brass rings collected in November 2006. Soil cores were placed on a tension table constructed from washed sand and the water level increased to bring the cores to saturation. Initial water repellence was overcome by allowing the cores to equilibrate for 3 weeks at saturation at the soil surface until no dry soil could be observed. A small depth increment of soil (approx 5 mm) was removed from the surface of the soil core to determine water content gravimetrically. The water potential was then decreased by lowering the hanging water column and adjusting this to equilibrate to the water potential at the centre of the next depth increment to be sampled for water content. Water potentials of 1, 2, 3, 4, 5, 7.5, 10, & 50 cm were generated in this way. Water filled porosity at 100cm potential was determined from samples placed in conventional pressure plate apparatus. The capillary equation (Eq 4) was used to convert the water filled porosity at each water potential to a fraction by area occupied by each pore size class, assuming a soil-water contact angle θ of zero.

A range of functions were fitted to the cumulative porosity vs pore size data with the aim of finding a distribution function (cdf) for the cumulative porosity.

2.3. Hydraulic conductivity

Hydraulic conductivity was determined at a range of high water potentials using field tension infiltrometers at potentials of 1, 2, 3, 4, 5, 7.5 and 10 cm of water. Soils were pre-wet prior to measurement using surfactants to break down water repellence. Saturated conductivity was determined using a single-ring infiltrometer prior to the tension infiltrometer measurements. Two replicates of the above measurements were made in November 2006 in the East Kiewa Research Catchments (Sheridan *et al.* 2007). Visual inspection of the measurement points following conductivity measurements revealed little evidence of water repellence, suggesting the use of surfactants was successful in this case. Measurement locations were prepared by removal of vegetation and litter, removal of some surface soil to produce a level area on the sloping land, and construction of a pad of commercially available washed garden sand for contact material. Laboratory testing of the contact material found that the air entry suction was greater than the maximum 10 cm water potential applied in this experiment. Recordings of conductivity were continued until steady values were observed.

Conductivity was quantified as the slope of the linear portion of the plot of cumulative infiltration against cumulative time. Water potential values were converted to an equivalent pore size using Eq 4. Measured conductivity values were expressed as a proportion of the saturated conductivity, and are referred to herein as the relative conductivity K_r. The plot of K_r ($0 \le K_r \le 1$) against pore diameter d can be represented as a cumulative distribution function (cdf) and therefore the proportion of total conductivity at saturation between pore sizes d_1 and d_2 can be determined from $K_r(d_2) - K_r(d_1)$.

2.4. Contact Angle

The contact angle of the soil was determined using the method described by Letey *et al.* (1962). These authors derive a flow equation by assuming that the soil can be represented as a collection of tubes, through which flow obeys Poiseuille's equation

$$Q = \frac{\pi r^4 P}{8 L \eta} , \quad (1)$$

where Q is the flow rate (L^3 T^{-1}), r is the pore radius, L is the pore length, & η is the viscosity of the solution. Pressure P includes both gravity, P_g, and capillary, P_c , components

$$P = P_c + P_g . \quad (2)$$

P_g is given by the hydrostatic pressure equation

$$P_g = \rho g h \quad (3)$$

where ρ is the solution density, g is the acceleration due to gravity, & h is the pore length plus the depth of the solution above the capillary. P_c is determined from the capillary equation

$$P_c = \frac{2\gamma \cos\theta}{r} \quad (4)$$

where γ is the solution surface tension, and θ is the contact angle between the solution and the solid surface (eg. the soil). Substituting Eqs 3, 4 and 2, into Eq 1 gives

$$Q = \frac{\pi r^3 (\rho r g h + 2\gamma \cos\theta)}{8 L \eta} . \quad (5)$$

Eq 5 is then divided by the cross sectional area of the effective pore (πr^2) to express the flowrate as a depth per unit time (L T^{-1}), and then multiplied by the porosity C to give the flowrate Q" for a collection of pores of effective radius r

$$Q'' = \frac{Cr(prgh + 2\gamma \cos\theta)}{8 L \eta} . \quad (6)$$

When water is used as the percolating solution, Eq 6 includes two unknowns; the contact angle θ and the effective pore radius r. However, by using 99% ethanol as the percolating solution, for which the contact angle with soil in air can be reasonably assumed to be zero, Eq 6 can be solved for r. This known value of r is then used to solve for the soil-water contact angle when water is used as the percolating solution on other cores packed in the same way. The units and values for the physical quantities listed above are given in **Table 1**.

Table 1. Physical quantities, units and values for soil physical calculations.

Physical quantity	Units	Value
General		
Porosity C	na	0.80
Gravity g	ms^{-2}	9.8
Ethanol		
Contact angle θ	degrees	0
Surface tension γ	Nm^{-1}	0.0223
Viscosity η	kg $m^{-1}s^{-1}$	0.00106
Density ρ	kg m^{-3}	790
Water		
Surface tension γ	Nm^{-1}	0.0728
Viscosity η	kg $m^{-1}s^{-1}$	0.000891
Density ρ	kg m^{-3}	1000

Soils were collected from an unburnt area from six locations to a depth of 20mm in December 2006 in a water repellent condition. Samples were sieved to yield a sample less than 500µm and greater than 300µm diameter. The laboratory column was 0.026 m diameter and the soil depth was 0.12m and the solution head depth was varied from 0.025 to 0.098m using a constant head device. It should be noted that this method does not measure the *initial* contact angle prior to the wetting of the soil.

2.5. Modelling runoff generation

Computer simulations of infiltration-excess runoff under 100 mm h^{-1} rainfall were generated from plots the same dimensions as the field rainfall simulation plots (1.5m wide by 2, 1, 0.5, 0.25, and 0.125m long). Representative pore size values were randomly allocated to each $1cm^2$ grid cell using the cumulative porosity function fitted to the measured porosity data.

The hydraulic conductivity function $K_r(d)$ was then used to calculate the proportion of the total saturated hydraulic conductivity for each grid cell based on the pore size of that cell d_1 and the cell with the next highest pore size d_2 using the function $K_r(d_2) - K_r(d_1)$.

Rainfall was then applied at 100 mm h^{-1} and the cumulative runoff calculated for each strip of cells assuming linear flow down the plot. The runoff rate (mm h^{-1}), the area (m^2) connected by overland flow-paths to the plot outlet, and the average length of these connections (mm), was then

calculated. Monte Carlo simulations of the spatial grid were not used as each of the 150 strips of cells provided an independent measure of the above outputs.

To simulate the effect of increasing water repellence on runoff generation, the capillary equation (Eq 4) was solved for r to determine the minimum radius at which water would enter under a 1mm head depth (ie. $P_c = 0.001$m)

$$r = \frac{2\gamma \cos\theta}{P_c} \quad . \qquad (7)$$

Infiltration was then excluded from pores less than this critical radius, and the total saturated conductivity for the plot reduced accordingly. This modified grid of values was then generated and runoff and connected area calculated as for the non-water repellent case (described above). This approach does not account for the reduced infiltration into the remaining pores where the pressure entry value is exceeded by the 1mm head.

2.6. Measuring runoff generation

Runoff was measured from 1.5 m wide by 2.0 m long plots subjected to 100 mm h^{-1} rainfall. Runoff was measured for 30 min then the plot length reduced in stages to 1.0, 0.5. 0.25, and 0.12 m and runoff measurements repeated until steady state was reached. Measurements were made during summer under water-repellent conditions and during winter under non water-repellent conditions. The observed changes in runoff as a function of water-repellent status and plot length were compared to model results under similar conditions.

3. RESULTS

3.1. Pore size distribution

The relationship between pore diameter and cumulative porosity $C_c(d)$ (Figure 2) was log-linear with linear regression yielding the following best fit with d (μm)

$$C_c(d) = aLn(d) + b \qquad 0 \le C_c(d) \le 1 \qquad (8)$$

where a and b are fitted parameters. The values for a and b were 0.160 and 0.292 respectively. Solving for $C_c(d) = 0$ and $C_c(d) = 1$ implies that $6.2 \le d \le 3215$, which is not realistic at a hillslope scale (which includes tree root holes >> 3215 um), but was considered adequate for the purposes of this study.

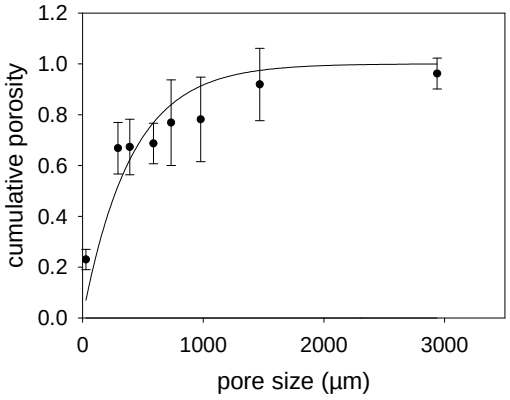

Figure 2. The relationship between pore diameter (μm) and cumulative porosity $C_c(d)$. Error bars on data points are +/- 1 SD; the line is fitted by least squares regression.

The total porosity of 78% measured at the experimental site initially appeared unreasonably high. Comparison with literature values shown in Table 2 suggests the values measured in this study are comparable with the results of others working with forest soils of this type.

Table 2. Total soil porosity (%), macro-porosity, micro-porosity, and bulk density (g cm^{-3}) results from this study compared to Victorian forest soil measurements from the literature.

	This study	Top Regen[B]	Simpsons Rd[B]	Deception Spur[A]	LCC[C]	Old Mill[A]
Total[D]	78	71	62	69	68	66
>30um	32	23	13	24	25	24
<30um	46	48	49	45	43	42
BD	.86	.53	.94	.75	.85	.69

>30um classed as macro-porosity, <30um as micro-porosity
[A] Rab et al (1994); [B] Rab et al. (1996); [C] Unpublished data from Long Corner Creek; [D] note that these values are fractions of the total soil volume.

3.2. Hydraulic conductivity

The relationship between pore size d and the relative conductivity was represented by the linear function shown in Figure 3 (Eq 9). This function was fitted so that d did not exceed the maximum pore size given by Eq 8

$$K_r(d) = d/3054 - 0.05 \qquad 0 \le Kr(d) \le 1 \; . \qquad (9)$$

Alternative functions with a more physical basis were tried (Moore *et al.* 1986; Wilson & Luxmoore 1998) though failed to fit the data at the larger pore size end of the range. The linear function fit the larger pore size data well, while the lack of fit for the smallest pore sizes will introduce only small error as the relative contribution to saturated conductivity of these pores is small.

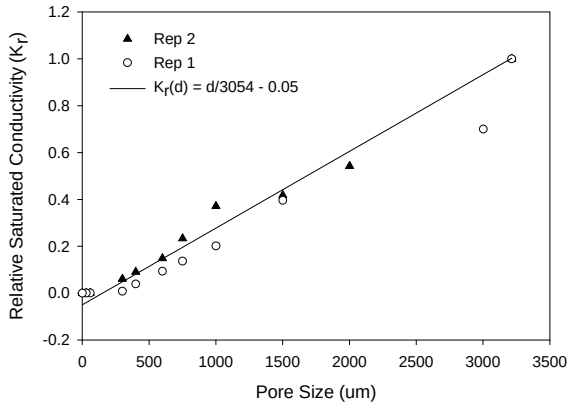

Figure 3. The relationship between pore size (μm) and relative saturated hydraulic conductivity K_r for two replicates under non-water repellent conditions were the contact angle is assumed to be zero.

3.3. Contact angle

The infiltration rate Q" determined using *ethanol* as the percolating solution was 1.17 x 10^{-3} m s^{-1} , yielding an effective pore radius *r* of 220 μm. The infiltration rate Q" determined using *water* as the percolating solution was 0.775 x 10^{-3} m s^{-1} , yielding a soil-water contact angle θ of 90.3 degrees. Assuming a 1mm layer of water on the soil surface during ponding, then the minimum water conducting pore would have a radius of 77 μm based on Eq 7.

3.4. Runoff generation

The cumulative porosity distribution function $C_c(d)$ is therefore given by

$$C_c(d) = \begin{cases} 0 & for\ d < 0 \\ 0.16\,Ln(d) + 0.292 & for\ 0 \le d \le 3215 \\ 1 & for\ d > 3215 \end{cases} \quad (10)$$

and the cumulative relative conductivity distribution function $K_r(d)$ is given by

$$K_r(d) = \begin{cases} 0 & for\ d < 0 \\ d/3054 - 0.05 & for\ 0 \le d \le 3215 \\ 1 & for\ d > 3215 \end{cases} \quad .(11)$$

Table 3 lists the results from computer simulations of plot infiltration and runoff properties for a soil with 309 mm h^{-1} infiltration capacity during 100 mm h^{-1} rainfall for a range of soil-water contact angles, including but not limited to the value determined from the laboratory contact angle measurement.

The results show that:

- Under non water-repellent conditions only a small fringe adjacent to the plot outlet contributes runoff to the plot exit;
- Both the runoff rate and the average connected length (with the plot outlet) are very sensitive to the selected contact angle;
- 20% runoff can be generated even when the infiltration capacity (127 mm h^{-1}) is higher than the rainfall rate (100 mm h^{-1}).

Table 3. Computer simulations of plot infiltration and runoff properties for a soil with 309 mm h^{-1} infiltration capacity during 100 mm h^{-1} rainfall for a range of soil-water contact angles.

Property	Non-water repellent		Water repellent	
	Contact angle (degrees)			
	0	**90.3**	**94**	**95**
Infiltration capacity[A]	309	300	127	78
Infiltration rate[B] (100 mm h^{-1} rain)	99	98	80	53
Runoff rate (100 mm h^{-1} rain)	1	2	20	47
Mean connected length[C] mm	32 (46)	67 (105)	715 (567)	1543 (462)
Connected area[D] (m^2)	0.05	0.1	1.1	2.3

A; the net infiltration capacity of the plot. B; the difference between rainfall and runoff. C; the average length of overland flow paths connected with the plot outlet. D; total area of all overland flow paths connected to the plot outlet.

Computer simulations of runoff were compared to runoff values measured using field rainfall simulation during both water repellent and non-water repellent conditions (Figure 4). These field

results do not offer a direct comparison with the modelled data as the infiltration capacity at the time of the rainfall simulation was different to the infiltration capacity measured at the time of the field tensiometer measurements. The field results do however allow a comparison of the trends in runoff patterns under differing conditions of plot length and water repellence.

The results show that the modelled runoff was able to replicate the patterns of observed runoff for a range of plot lengths and water repellent levels, however the absolute magnitude of runoff was found to vary between the model and the observed data for the reasons outlined above.

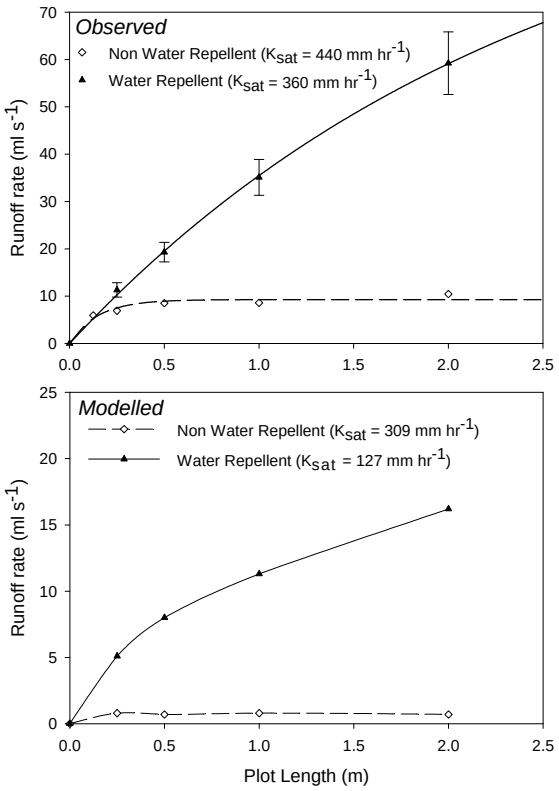

Figure 4. The effect of water repellence on runoff rates (ml s^{-1}) as a function of plot length, a) as observed during field rainfall simulation, and b) modelled output using the method described in this paper. Note differences in vertical axis scale.

4. DISCUSSION

4.1. Do the results support the hypothesis?

When the laboratory measured contact angle of 90.3^{o} is used in the runoff model, runoff generation is increased only slightly in summer (Table 3) and the modelled results do not support the experimental hypothesis. However if it is assumed that the field soil-water contact angle increases to 94^{o} in summer, then the results support the hypothesis that the observed spatial and temporal patterns of infiltration and runoff generation can be attributed to seasonal changes in water repellence. Several technical and theoretical issues may have bearing on the conclusions drawn in this paper.

Firstly, the method used for determining the contact angle in this paper involved repacked laboratory columns of sieved soil. This method may have introduced errors into the calculation of the contact angle, including the breaking up of water repellent fungal hyphae. However, Sheridan *et al*. (2007) showed that extreme water repellence could be generated in this soil when crushed to <2mm simply by oven drying below a water content threshold. It is proposed that future experiments for measuring the contact angle utilise a similar theoretical approach, except that the measurements are made in-situ under field conditions, possibly using tension infiltrometers as well as positive pressure apparatus.

Secondly, the validity of the application of the capillary equation (Eq 4) for calculating critical pore entry pressures (Eq 7) in soil has been recently challenged by Shirtcliffe *et al.* (2006) on the basis of the limitation of assuming that soil is reasonably represented as a bundle of capillary tubes. Using an alternative assumption that the soil is better represented as a collection of close packed spheres the authors show that the critical soil-water contact angle may be as low as 50^{o}, resulting in serious errors in the calculation of wetting behaviour based on the current assumptions.

Lastly, the modelled results are very sensitive to the measured values of both porosity and conductivity for large pore sizes. Current methods used for quantifying these properties are at the technical limits of the equipment used (eg. the resolution of the tension infiltrometers at water potentials close to zero cm of water) and at the theoretical limits of the underlying assumptions. For example, the capillary equation (Eq 4) is derived assuming laminar flow in pores (ie. a Reynolds number of < 1000-2000). It is likely this value is exceeded for the pore sizes of interest at saturation in these highly porous forest soils.

4.2. Implications for modelling

Despite these issues, the results provide some valuable insights that have the potential to improve the prediction of infiltration excess runoff, soil erosion, and stream water quality. The concept of the connected area, that is the total landscape area that is *connected by overland flow paths* to the plot

outlet is particularly valuable as an input to soil erosion models. For example, sediment generation rates are typically described as functions of the total input energy, in turn a function of the energy input rate per unit area, and the total area. However, for constituents delivered by infiltration excess overland flow to a lower boundary such as a stream edge, it is the *hydrologically connected* area that is of interest, rather than the total area. This distinction is particularly important in landscapes where the net infiltration capacity is very high such as in wet Eucalyptus forests. As shown in Table 3, the connected area varies considerably at different times of the year depending on the assumed level of water repellence.

It should be noted that the above discussion only describes the area that is hydrologically connected via infiltration-excess overland flow. Saturation-excess overland flow may also may also provide an overland flow connection, and it is the combination of these two processes that will determine the net area connected to the stream edge by overland flow paths.

5. CONCLUSION

The aim of this research was to test the hypothesis that the unusual runoff and infiltration results reported by Sheridan *et al.* (2007) were due to strong water repellence resulting in very high spatial variability in conductivity, with a large proportion of soil surface area having zero to very low conductivity, punctuated by small areas of extremely high conductivity.

When the laboratory measured contact angle of 90.3^{o} was used in the runoff model, runoff generation was increased only slightly in summer and the modelled results do not support the experimental hypothesis. However if it was assumed that the field soil-water contact angle increased to 94^{o} in summer, then the results support the hypothesis that the observed spatial and temporal patterns of infiltration and runoff generation can be attributed to seasonal changes in water repellence resulting in the above described surface characteristics.

Further work and new methods are required to explore the relationship between the soil-water contact angle, soil infiltration capacity, and runoff generation for highly macroporous forest soils.

6. REFERENCES

Letey, J., Osborn, J. and Pelishek, R.E. (1962), Measurement of liquid-solid contact angles in soil and sand, *Soil Science,* 93(3), 149-153.

Moore, I.D., Burch, G.J. and Wallbrink, P.J. (1986), Preferential flow and hydraulic conductivity of forest soils, *Soil Science Society of America journal*, 50, 876-881.

Morbidelli, R., Corradini, C. and Govindaraju, R.S. (2006), A field scale infiltration model accounting for spatial heterogeneity of rainfall and soil saturated conductivity, *Hydrological processes,* 20, 1465-1481.

Rab, M.A., (1994), Changes in physical properties of a soil associated with logging of *Eucalyptus regnans* forest in southeastern Australia, *Forest Ecology and Management,* 70, 215-229.

Rab, M.A., (1996), Soil physical and hydrological properties following logging and slash burning in the *Eucalyptus regnans* forest of southeastern Australia, *Forest Ecology and Management*, 84, 159-176.

Shakesby, R.A., Doerr, S.H. and Walsh, R.P.D. (2000), The erosional impact of soil hydrophobocity: current problems and future research directions, *Journal of Hydrology,* (231-232), 178-191.

Sheridan, G.J., Lane, P.N.J. and Noske, P.J. (2007), Quantification of hillslope runoff and erosion processes before and after wildfire in a wet Eucalyptus forest, *Journal of Hydrology 343, 12-28.*

Shirtcliffe, N.J., McHale, G., Newton, M.I., Pyatt, F.B., and Doerr, S.H. (2006), Critical conditions for the wetting of soils. *Applied Physics Letters,* 89, 094101.

Wilson, G.V. and Luxmoore, R.J. (1988), Infiltration, macro porosity , and mesoporosity distibutions on two forested watersheds, *Soil Science Society of America journal*, 52, 329-335.